Learning Process for Reducing Uncertainties on Network Parameters and Design Margins

E. Seve, J. Pesic, C. Delezoide, S. Bigo, and Y. Pointurier

***Abstract*—In this paper, we propose to lower the network design margins by improving the estimation of the signal-to-noise ratio (SNR) given by a quality of transmission (QoT) estimator, for new optical demands in a brownfield phase, based on a mathematical model of the physics of propagation. During the greenfield phase and the network operation, we collect and correlate information on the QoT input parameters, issued from the established initial demands and available almost for free from the network elements: amplifiers output power and the SNR at the coherent receiver side. Since we have some uncertainties on these input parameters of the QoT model, we use a machine learning algorithm to reduce them, improving the accuracy of the SNR estimation. With this learning process and for a European backbone network (28 nodes, 41 links), we could reduce the QoT inaccuracy by several dBs for new demands whatever the amount of uncertainties of the initial parameters.**

***Index Terms*—Machine learning; Network optimization; Optical networks; Supervised learning.**

I. Introduction

Efficiency and optimization is mandatory for network operation to support the exponential increase of network traffic and keep network design costs within reasonable limits. Among all possibilities to optimize network cost, we can, for example, leverage finer granularity optical transponders [1,2] or manage the spectral power to better use the available margins in the network [3]. Many other techniques also exist in the literature [4,5]. Another way to operate a network more efficiently is to improve the knowledge of the network by automatically collecting network information over time and analyzing this information with the help of big data or machine learning techniques. Doing this will lead to more accurate network design and thus lower margins [6–9].

The design of optical networks always relies on a software tool to predict the signal-to-noise ratio (SNR) for all traffic demands (i.e., quality of transmission, or QoT) to ensure that the quality of a signal carried on a light path is above a predefined threshold. Any QoT model typically is based on a physical model with input parameters describing network elements. To ensure that all traffic demands in an optical network fulfill their target capacities, network designers add significant (up to several dBs) pre-defined "design margins" to the values predicted by the QoT model or tool [4,5]. A significant amount of margins—design margins—are added to compensate for prediction errors of the QoT model, resulting in network over-dimensioning. Design margins compensate for errors both from the QoT model itself and from the uncertainties of the QoT model input parameters. The latter comes from the incomplete knowledge of the actual parameters of deployed network elements. By measuring some of the most sensitive optical layer parameters, it is possible to improve that knowledge and thereby save unnecessary margins.

Correlating information collected from a set of already established demands to estimate the QoT of new demands has been investigated with various methods. An approach based on machine learning techniques has been developed in [10,11]. In [10], the learning process is fed by a set of network features (i.e., number of links, total length, longest link length, traffic volume, and modulation format) and the output is a binary variable indicating whether the bit error rate is lower than the system threshold. In [11], the learning process is fed by the signal power, the number of spans, the baud rate, and the channel spacing. A mapping function relating the demand feasibility [10] or the bit error rate [11] and all the network parameters is learned and can be used to classify or predict the performance of any new demand, knowing all the features' values. The approach used in [10] is based on the Random Forests classifier method, while in [11], a method based on a Gaussian process regression was considered. Neither of these two studies uses any predefined model of the propagation physics; the model itself is learned from measurements with initial demands and during the network operation.

QoT estimators based on models of propagation physics have been developed and validated for many years [12–18]. It is also wise to use the information available in these models. All recent models assume that nonlinear distortions can be approximated by additive Gaussian noise. The inverses of the SNR evaluated in all spans can be added to give the inverse of the total SNR for any light path in dispersion unmanaged fiber networks [12–18].

However, there is always a discrepancy between the QoT estimation given by these models and the actual values.

Manuscript received August 15, 2017; revised November 27, 2017; accepted December 7, 2017; published February 1, 2018 (Doc. ID 303001).

The authors are with Nokia Bell Labs, Nozay, France (e-mail: emmanuel.seve@nokia-bell-labs.com).

https://doi.org/10.1364/JOCN.10.00A298

Therefore, we can learn from the measurements to refine the QoT estimation. There are two options to reduce this discrepancy.

The first one is to learn the values of the SNR for all links of the network by correlating the measured SNR collected from a set of already-established demands. We can then predict the QoT of new demands with a reduced inaccuracy. This method has been considered for a full spectrum occupation using network kriging or norm l_2 minimization [19]. Then, the network kriging technique used in Ref. [19] has been updated to deal with a realistic wavelength allocation with nonlinear interactions between demands, accounting for the actual interference of the light paths, and thus yielding more accurate QoT estimations [20]. Moreover, the degradation that the new light path causes to the existing ones can be considered. It is in this context that the first experimental demonstration of a learning process was implemented in Refs. [21,22] with a six-node network and open ROADMs that constantly monitor the performance of established demands. The accuracy of the SNR estimation for new light paths has been improved by learning the SNR of each of the links that compose them.

The method we propose here also stems from considerations on the physics of propagation, but it is different from Ref. [19–22] in the sense that we do not reduce the uncertainty of the SNR estimation but that of the input parameters of a QoT model by leveraging SNR measurements from coherent receivers terminating previously established light paths. The paper is organized in five sections. In Section II, we describe the general learning process used to reduce uncertainties on the input parameters of any QoT model. In Section III, we discuss the two models we have used to estimate the QoT of optical demands—each having its own limitations and advantages. In Section IV, we present the setup of our simulations and all assumptions for the numerical study. Finally, in Section V we describe all results obtained on the improvement of the QoT estimation.

II. Learning Process

Figure 1 shows the complete network design cycle. For the deployment of initial demands (greenfield planning, Fig. 1, left), we first allocate the needed resources (links, wavelengths) using a QoT estimator based on a mathematical model of the physics of propagation to ensure errorless reception (after forward error correction, or FEC). However, due to all uncertainties on the network parameters, the actual QoT can turn out to be smaller than the value predicted by the mathematical model (estimated QoT) and may be poorer than the FEC limit. To avoid this situation, operators require system vendors to design their networks with a better QoT than predicted by the model, by an amount often called the design margin (m in Fig. 1) [4,5]. The actual value of m depends on the operators and on the vendors, and can easily reach several dBs in Q^2 dB-factor units. In this paper, we vary the value of m to cover typical cases. Today, this value is set once and for all across the lifetime of the network: the design margin for new demands (m' in Fig. 1) is then unchanged (see the red arrow in Fig. 1, $m' = m$), when new demands must be allocated.

We are proposing the addition of a training step between the greenfield and brownfield planning to reduce the uncertainty on some input parameters of the QoT model using a machine-learning algorithm, which will be explained in further detail. After light paths for initial demands are established (Fig. 1, Deployment phase), we collect all the monitored data issued from direct field measurements. Our machine-learning algorithm provides refined input parameters for the QoT model with a reduced uncertainty, leading to an improvement in the QoT prediction for all new demands (Fig. 1, Prediction phase). The design margin m' may be lower than the margin m used for the initial demands. This learning process applies to dynamic networks since it can be performed at any moment during the life of the network, when a demand is added or removed.

The block diagram of our machine-learning algorithm based on a gradient descent algorithm is shown in Fig. 2. Since this study is completely numerical, the first three blocks show the emulation of the actual values of the QoT for a real network.

First, we start by a routing and wavelength assignment (RWA) with a set of N_d initial demands (Fig. 2, 1). The RWA

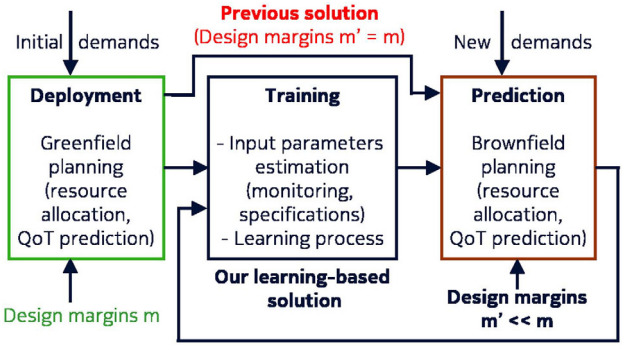

Fig. 1. Illustration of the complete network design cycle. Cycle consists of three phases: deployment, training, and prediction.

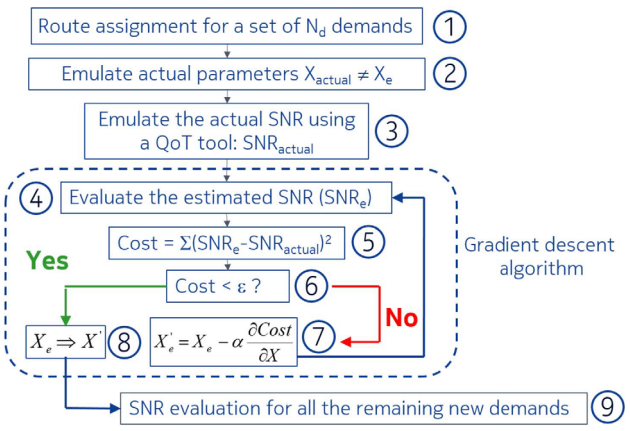

Fig. 2. Block diagram of the learning algorithm. X can be any input parameter of the QoT model.

process will be explained in more detail in Section IV. We emulate the actual values of the QoT parameters (X_{actual}) with a random set of values (Fig. 2, 2). In this study, we suppose that the QoT model gives the ground truth; the measured SNR (SNR_{meas}) for the initial demands is then emulated from the actual values of the QoT parameters using a QoT model and will be called $\text{SNR}_{\text{actual}}$ in the rest of the article (Fig. 2, 3).

To estimate the SNR of new demands before being established (SNR_e), we use the same QoT model as the one used to emulate the measured SNR of the initial demands. We have two options for the input parameters. For the first option, we extract the parameters from the data sheet specifications, using the settings defined during the initial network design. For the second option, we obtain the input parameters by monitoring some specific network parameters (e.g., fiber span loss, amplifier output power, digital signal processing issues). Even if the values of the input parameters obtained with the second option are more accurate, they still deviate from the actual ones, leaving some (reduced) uncertainty when predicting system performance for the new demands. Our final goal is to reduce this discrepancy between SNR_e and $\text{SNR}_{\text{actual}}$.

In this paper, we chose the second option and we monitor several input parameters of the QoT model. The values of these input parameters are named X_e; the index e means that we estimate them by monitoring or other means. We emulate X_e with a random set of values different from the set of actual values X_{actual}. The difference between the actual (X_{actual}) and estimated (X_e) values illustrates the measurement uncertainty. They are both generated with different random seeds and with a systematic shift between the average values to emulate a calibration error of the measurement tools.

All this information on the actual SNR ($\text{SNR}_{\text{actual}}$) and the measured values of the input parameters of the QoT model (X_e) are collected and feed a gradient descent algorithm (dashed box in Fig. 2). The process starts by estimating the SNR of all initial demands (SNR_e) using the QoT model with the monitored values X_e as input parameters (Fig. 2, 4). Since SNR_e is obviously different from the actual one ($\text{SNR}_{\text{actual}}$), we build a cost function $\text{Cost} = \Sigma(\text{SNR}_e - \text{SNR}_{\text{actual}})^2$ (Fig. 2, 5). The sum is made over all demands already established to correlate all the available network information. This cost function is minimized by iteratively modifying all the input parameters of the QoT tool (X_e) simultaneously (Fig. 2, 7). Once the cost function *Cost* converges toward a value smaller than a predefined threshold ε (Fig. 2, 6), the QoT tool can be used with the new values of the input parameters x' (Fig. 2, 8) yielding a reduced design margin ($m' < m$) for new traffic demands (Fig. 2, 9). With information coming from the new demand(s), the QoT prediction may be iteratively refined through retraining, as shown in Fig. 1. Finally, we assume that our QoT model itself is perfect and we focus on decreasing the input parameters' uncertainties. The uncertainty of the model, which is out of the scope of this article, will be included in a future study.

III. QoT Models

The machine learning process presented in this paper can be used to reduce the uncertainties on the input parameters of any QoT model. As an illustration, we will apply this process to two QoT models: the semi-analytical model for brisk assessment (SAMBA) of performance [18] and the extended Gaussian noise model (EGN) [23]. In the next section, we present these two models.

A. Analysis With the SAMBA Model

First, we briefly describe the model [18], renamed SAMBA, according to which the combined effect of chromatic dispersion and Kerr nonlinearity generates a nonlinear distortion after each of the N fiber spans, leading to a nonlinear SNR (SNR_{NL}) defined by

$$\text{SNR}_{\text{NL}} = 1/\sum_{k=1}^{N} P_k^2 \sigma_k, \tag{1}$$

where P_k is the channel average input optical power of the kth span and σ_k is the normalized nonlinear noise variance for span k. In the SAMBA model, σ_k is a function of the cumulated dispersion at the input of the fiber span, which is either numerically computed [18] or measured over all meaningful system configurations [24]. For an N-span system, noise accumulates according to a law by which the inverse of the total nonlinear SNR [Eq. (1)] is the sum of the inverse of the nonlinear SNR from all spans. This law stems from the assumption that the nonlinear noise distortion issued from any span is independent from the nonlinear distortions from all the other spans. This law holds well over dispersion unmanaged (DU) systems [24], which is the case for all recent networks.

Even though the above considerations apply to fiber systems of any inter-amplifier lengths, we further assume that transmission systems then have the same distance L between amplifiers to simplify equations (but without loss of generality for the remainder of the paper). In this case, if we consider that nonlinear noise and amplifier noise do not interplay, we can add the nonlinear noise to the amplifier linear noise (gauged by the optical SNR, or OSNR) and finally we can write the SNR of the whole light path as

$$\frac{1}{\text{SNR}} = \frac{1}{\text{OSNR}} + \frac{1}{\text{SNR}_{\text{NL}}}, \quad \text{with}$$
$$\frac{1}{\text{OSNR}} = h\nu \cdot B_{\text{ref}} \cdot e^{\alpha L} \sum_{k=2}^{N} \frac{\text{NF}_k}{P_k} = \sum_{k=1}^{N} A \frac{\text{NF}_k}{P_k}, \tag{2}$$

where NF_k is the noise figure of the amplifier in span k, α is the unitary fiber loss, L is the common fiber span length and N is the number of amplifier spans across the light path. The initial SNR ($k = 1$) is considered as infinite. We assume that all are known without any uncertainty. B_{ref} is the reference spectral bandwidth (i.e., 12.5 GHz), h is the Planck constant, and ν is the mean optical frequency. For a meshed optical network with N_d demands, we need to solve a system of N_d equations which can be written as

$$\frac{1}{\mathrm{SNR}_j} = \sum_{k=1}^{N_j} \left(\sigma_k^j P_k^2 + A \frac{\mathrm{NF}_k}{P_k} \right) \tag{3}$$

with $j \in [1, \ldots, N_d]$, where j is the index of the demand, and σ_k^j is the nonlinear variance of the kth span for demand j. This dependence on the index of the demand is due to the fact that the signal arrives at the input of the span k with a cumulated dispersion, which can be different from one demand to another since the history of crossed fibers may be different for each demand j. We can assume that coefficient A does not depend on the index of the demand since it corresponds to the linear distortion introduced by each amplifier.

B. Analysis With the EGN Model

The EGN model presented in detail in Ref. [23] has the advantage to be approximated by a closed form formula giving the nonlinear noise variance for one span and any wavelength allocation. This model can be expressed in the same form as in Subsection III.A with the semi-analytical model

$$\mathrm{SNR}_{\mathrm{NL}} = 1/\sum_{k=1}^{N} P_k^2 \sigma_k.$$

The normalized nonlinear distortion takes the following analytical form:

$$\sigma_k^j = \sum_{i=1}^{N_{\mathrm{ch}}} A_k \left[\operatorname{asinh}\left(C_k \left[f_i - f_j + \frac{B_i}{2} \right] B_j \right) \ldots - \operatorname{asinh}\left(C_k \left[f_i - f_j - \frac{B_i}{2} \right] B_j \right) \right]. \tag{4}$$

This expression is the sum of the contributions of all channels present in span k (including itself) on channel j. N_{ch} is the total number of channels. B_i is the baud rate of channel i. The terms A_k, B_i and B_j depend on the physical characteristics of the span k and their expressions can be found in Eq. (128) in Ref. [23]. The expression of the linear noise distortion (i.e., 1/OSNR) induced by the amplifiers is the same as in Subsection III.A.

C. Comparison Between the SAMBA and EGN Model Assumptions

The main advantage of the SAMBA model over EGN is that it accounts for the dependence of nonlinear noise with the cumulated dispersion at the span input. This advantage can be particularly meaningful over low dispersion fiber (e.g., less than 5 ps/nm/km) and moderate distances (e.g., shorter than 500 km). The closed-form expression of the EGN model [i.e., Eq. (4)] assumes that the nonlinear distortions induced by each span are independent and so the dependence on the cumulated dispersion at the span input is overlooked. EGN is then qualified as incoherent and will give the same estimated SNR whatever the span order. A coherent version of the EGN exists but cannot be expressed in a closed form.

However, as opposed to the early version of the SAMBA model of Ref. [18] used as benchmark here, the EGN model can easily capture the actual wavelength allocation plan of optical channels to refine the accuracy of its light path feasibility predictions. The SAMBA model assumes a worst-case scenario of channel loading. With the EGN model, we can estimate the SNR for any wavelength allocation.

The assumptions of the learning process are summarized in Table I for the two QoT models: SAMBA and EGN.

TABLE I
ASSUMPTIONS OF THE LEARNING PROCESS FOR THE SAMBA AND THE EGN MODELS

QoT Model	Cumulated Dispersion (Span Order)	Wavelength Allocation
SAMBA	Simple numerical evaluation	Computation for each wavelength allocation
EGN	No simple expression	Built-in dependence on wavelength allocation

IV. SIMULATION SETUP AND ASSUMPTIONS

In this study, we consider the European backbone network consisting of $M = 28$ nodes, 41 uncompensated bidirectional links and $N = 258$ standard single-mode fiber (SMF) spans [25]. The network topology is presented in Fig. 3. The number on each link corresponds to the number of spans between two nodes, expressed as multiples of 100 km. Each demand is carried by one wavelength and the signal is modulated at 28 Gbaud with a PDM-QPSK modulation format, yielding 100 Gb/s net bit rate. For this topology, the maximal number of unidirectional demands is equal to $M \times (M - 1) = 756$. We emulate a uniform traffic matrix with only one demand between each pair of nodes

Fig. 3. European backbone network topology consisting of $N = 28$ nodes, 41 dispersion uncompensated bidirectional links, and 258 standard SMF spans [25]. The number on each link corresponds to the length between two nodes as a multiple of 100 km.

and one wavelength per demand. For the RWA, we use a Dijkstra algorithm to find the shortest path and the first-fit rule for wavelength allocation: when a new demand must be established, we search the first empty wavelength slot for all links along the light path. With a different RWA, the algorithm of our learning process would be identical since only the computation of the nonlinear variance σ_k^j is affected. In the same way, there is no change in the algorithm when considering removed demands in a fully dynamic light path establishment.

In addition to the limitations inherent to each QoT model presented in Section III, we list the assumptions common to both QoT models. First, all demands are carried transparently; optimization of regenerator position is out of the scope of this paper. We assume that all fiber span input powers are designed to be identical at P_0 over each of the 258 SMF spans in the network (but are not strictly the same, due to realistic implementation and measurement errors). This is a reasonable target design choice considering that all spans have the same length. We assume that amplifier gain is perfectly flat. Non-zero excursion of power levels across the spectrum multiplex is out the scope of this paper and will be the subject of future work.

The inaccuracy of the QoT estimation is essentially due to the uncertainties on two input parameters of the QoT model: the input power level at the input of each span (how much it deviates from the target setting P_0) and the noise figure (NF) of each network amplifier. As explained in Section II, we emulate the actual (and measured values of all input parameters. The actual values $\{X_{\text{actual}}\}$ are reported in the second column in Table II. The set of input powers $\{P_{\text{actual}}\}$ has a normal distribution $N(\mu_p, \sigma_p)$ and the set of noise figures $\{\text{NF}_{\text{actual}}\}$ has a uniform distribution $U[\min, \max]$. The actual values of the SNR $\{\text{SNR}_{\text{actual}}\}$ are then evaluated using Eq. (2) for the SAMBA model or Eq. (4) for the analytical EGN model. The estimated values are reported in the last column of Table II. For the estimated input powers $\{P_e\}$ (emulating measurements), we tested our learning process with different values of μ_p to emulate a systematic shift of the power measurement caused by imperfect equipment calibration. The statistical error due to the measurement itself is determined by the value of σ_p. The measured power can be different from one span to another, due to amplifier gain fluctuation and/or due to a difference of span loss. For the noise figure, we use values coming from the amplifiers' data sheets, either $\{\text{NF}_e\} = 5$, 6, or 7 dB. The training phase of the learning process is realized with various numbers of demands: $N_d = 50$, 100, 200, 400, or 600, and we assess the new and more accurate QoT model (i.e., with reduced uncertainties on input parameters) by predicting the SNR for each of the remaining 756-N_d demands, namely $\{\text{SNR}_e\}$. It means that we consider a dynamic light path establishment with only new demands, the demands used for the training step are not extracted. The analysis of the statistics of the SNR error (i.e., $\text{SNR}_e - \text{SNR}_{\text{actual}}$) is provided in Section V.

TABLE II
ACTUAL AND MEASURED VALUES FOR THE INPUT POWER AND THE AMPLIFIERS' NOISE FIGURE

QoT Input Parameters	Actual Values	Estimated Values
Input power	$\{P_{\text{actual}}\}$	$\{P_e\}$
	$N(\mu_p, \sigma_p)$	$N(\mu_p, \sigma_p)$
	$\mu_p = 0$ dBm	$\mu_p = [-2, -1, 0, 1, 2]$ dBm
	$\sigma_p = 1$ dBm	$\sigma_p = 1$ dBm
Noise figure	$\{\text{NF}_{\text{actual}}\}$	$\{\text{NF}_e\}$
	U [5,7] dB	5, 6, or 7 dB

V. RESULTS

A. Semi-Analytical QoT Model (SAMBA)

In Fig. 4, we plot the error probability on the SNR prediction ($\text{SNR}_e - \text{SNR}_{\text{actual}}$) with learning (solid line) and without learning (dashed line) for the establishment of each demand not in the training set (i.e., for each of $756 - 600 = 156$ demands). We choose one configuration of seed parameters: $\mu_p = 0$ dBm, $\text{NF}_e = 6$ dB, and $N_d = 600$. The benefit of the learning process is very visible since the width of the SNR error distribution almost vanishes after the convergence of the learning process: the distribution is strongly shrunk, with an average around 0 dB. To quantify more accurately the design margins after the learning process, we plot in a subset the error histogram obtained with learning with a 100× zoom. The SNR error reaches ±1 dB ($m = 1$ dB) without learning and is reduced to ±0.013 dB ($m' = 0.013$ dB) thanks to the learning process. Clearly, the QoT model is much more accurate for new demands, thanks to the learning process, suppressing almost all the input parameter uncertainties.

In Fig. 5, we further show all tested configurations of $\{P_e\}$ and $\{\text{NF}_e\}$. Each subfigure corresponds to one value of the systematic power shift μ_p. The vertical bar represents the 3σ-spread of the SNR error prediction for one demand among all the remaining demands. The x-axis represents the varying number of demands in the training set (i.e., today with already-established demands) from 0 to 600. Zero demand means that there is no training. For each number of demands, we show a group of three vertical bars, one for each NF_e value. Without the learning process,

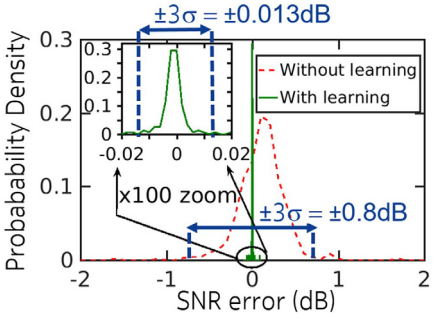

Fig. 4. Probability density of the SNR prediction error with learning (solid line) and without learning (dashed line). $\mu_p = 0$ dB, $\text{NF}_e = 6$ dB, and $N_d = 600$. The inset is a 100× zoom of the SNR error scale for the histogram obtained with learning (QoT model: SAMBA).

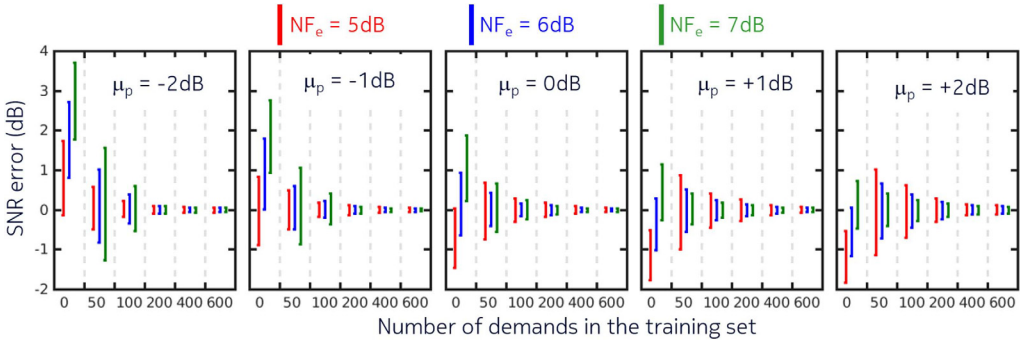

Fig. 5. Range of the SNR prediction error (mean $\pm 3\sigma$) for one demand among all the remaining demands as a function of the number of demands N_d in the training set and for five values of systematic power shift μ_p: −2 to +2 dB. The three error bars for each size of the training set correspond to various estimated noise figures NF$_e$: 5, 6, and 7 dB, respectively. Zero demand means that there is no training (QoT model: SAMBA).

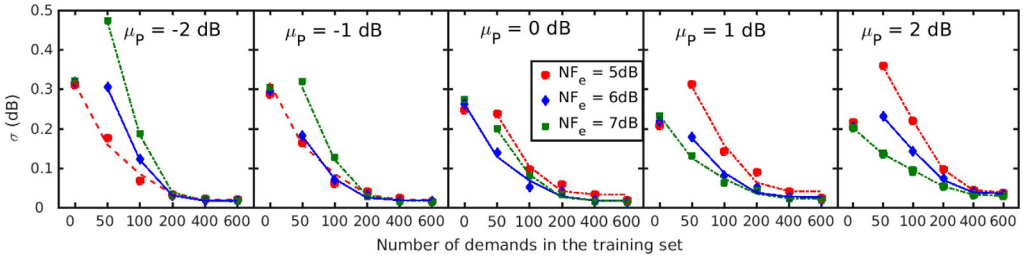

Fig. 6. Standard deviation as a function of the number of demands N_d in the training set and for five values of systematic power shift μ_p: −2 to +2 dB. The red dashed, blue solid, and green dot-dashed lines correspond to estimated noise figures NF$_e$ of 5, 6, and 7 dB, respectively. The points are the values of the standard deviation obtained after the learning process, and the lines are the corresponding exponential fitting curves (QoT model: SAMBA).

the SNR error varies between +3.7 dB and −1.8 dB (i.e., $m = 1.8$ dB). These values of the design margins, which are larger than the one reported in Ref. [5], are the result of a larger amount of uncertainties on the QoT tool input parameters. We chose these extreme values to validate our learning process for cases where an operator has a large lack of knowledge in its network. Thanks to learning, the SNR error spread decreases progressively with the number of demands and finally reduces to ±0.1 dB with 600 demands in the training set (i.e., $m' = 0.1$ dB). This evolution of the SNR error is almost identical whatever the initial error on the measured powers and the estimated noise figure (NF$_e$). For all tested configurations, the average SNR error converges to almost 0 dB. Moreover, a learning process trained with only 200 demands provides a SNR prediction with ±0.3 dB accuracy.

After showing that the range of the SNR error is reduced and shifted around 0 dB when increasing the size of the learning process, we show in Fig. 6 the evolution of the standard deviation with the number of demands. Each subfigure corresponds to one value of the systematic power shift μ_p. The x-axis represents the varying number of demands in the training set. For each number of demands, we have three curves, one for each NF$_e$ value: red dashed line (NF$_e$ = 5 dB), blue solid line (NF$_e$ = 6 dB), and green dot-dashed line (NF$_e$ = 7 dB). The points are the values of the standard deviation obtained after the learning process and the lines are the corresponding exponential fitting curves. We can distinguish two parts in the evolution of the standard deviation σ. Until 50 demands, the average value of the SNR error is always reduced, but not necessarily the standard deviation. This increase of the standard deviation occurs only for values of estimated parameters leading to the largest under- or overestimation of the SNR without the learning process (see Fig. 5). Above 50 demands, the average value of the SNR error almost vanishes for all values of estimated parameters, and the standard deviation σ of the SNR error decreases exponentially.

B. Analytical EGN QoT Model

As mentioned in Section IV, we used the Dijkstra algorithm with a first-fit allocation rule. Figure 7 represents the wavelength allocation for all 41 (bidirectional) network links and for the different numbers of demands N_d: 50 (a), 100 (b), 200 (c), 400 (d), and 600 (e). Each black square indicates the wavelength position on the 50 GHz ITU-grid. Obviously, the average number of wavelengths per link increases with the number of demands: 3.9 ($N_d = 50$), 6.6 ($N_d = 100$), 13 ($N_d = 200$), 25 ($N_d = 400$), and 35 ($N_d = 600$).[1] In Fig. 8, we represent the evolution of the

[1]With the previous model, the number of demands was constant (9 channels) for all the demands and whatever the number of demands there were.

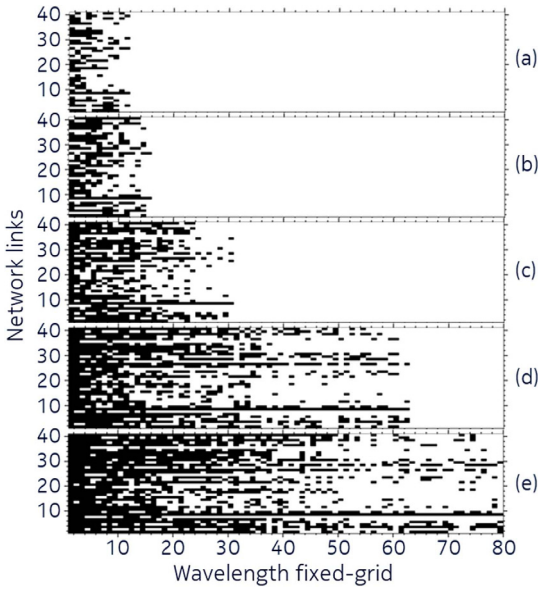

Fig. 7. Wavelength allocation for each of the 41 links of the network and for a different number of demands: 50 (a), 100 (b), 200 (c), 400 (d), and 600 (e). Each black square indicates the wavelength position on the 50 GHz ITU grid.

SNR error range with the number of demands in the same way as in Fig. 5 when there is no systematic error on the power measurement ($\mu_p = 0$ dBm). The vertical bars represent the 3σ-spread of the SNR error prediction for one demand among all the remaining demands. The x-axis represents the varying number of demands in the training set. Zero demand means that there is no training. For each number of demands, we have a group of three vertical bars, one for each NF_e value. The inset is a zoom for the three largest numbers of demands (200, 400, and 600). The main difference when compared to the results obtained with the SAMBA model is that we need to recalculate the wavelength allocation for each link when we add a new demand. The wavelengths assigned for the initial demands are unchanged, but the number of neighboring channels increases and, therefore, the normalized nonlinear variance σ_k^j [Eq. (4)] must also be re-evaluated for each link k and each demand j (both the initial and new demands).

Without the learning process, the error varies from −1.5 dB (for an underestimation of the estimated noise figure, $NF_e = 5$ dB) to +2 dB (for an underestimation of the noise figure, $NF_e = 7$ dB): $m = 1.5$ dB. When we include the learning process, the range of the SNR error decreases progressively with the number of demands in the training set. With the help of the zoom shown in the subfigure, we see that it is reduced to less than ±0.02 dB with 600 demands in the training set (i.e., $m' = 0.02$ dB). As in Fig. 5, we have also considered different values of the systematic error μ_p, and we have grouped these results in Fig. 8. Each inset corresponds to one value of systematic power shift μ_p (from −2 dB to +2 dB). Without the learning process, the SNR error varies between +3.1 dB and −4.2 dB (i.e., $m = 4.2$ dB). Thanks to the learning process, the SNR error spread decreases progressively with the number of demands and finally reduces to ±0.02 dB with 600 demands in the training set (i.e., $m' = 0.02$ dB). Here again, as with the SAMBA model, our method drastically reduces the error when predicting performance with the EGN model.

As seen in Fig. 5, this evolution of the SNR error is almost identical for all sets {measured powers, estimated noise figure (NF_e)}: the average SNR error converges to almost 0 dB. Again, a learning process trained with only 200 demands leads to a QoT tool with ±0.07 dB accuracy. In Subsection V.A, we obtained accuracy of 0.3 dB for 200 demands, showing again that a more precise QoT model does not imply a decrease of the prediction accuracy or new demands. Our method to decrease the design margin can then be applied with any QoT model.

VI. Conclusion

By feeding a learning process based on a gradient descent algorithm with a set measured/monitored data (SNR, power levels, noise figures), we have shown that it is possible to drive design margins down. In the brownfield scenario of a European backbone network, whatever the amount of uncertainties of the power levels and noise figures of the amplifiers, we computed a reduction of the QoT prediction error from 1.8 dB to 0.1 dB with the SAMBA model and from 4.2 dB to 0.02 dB with the

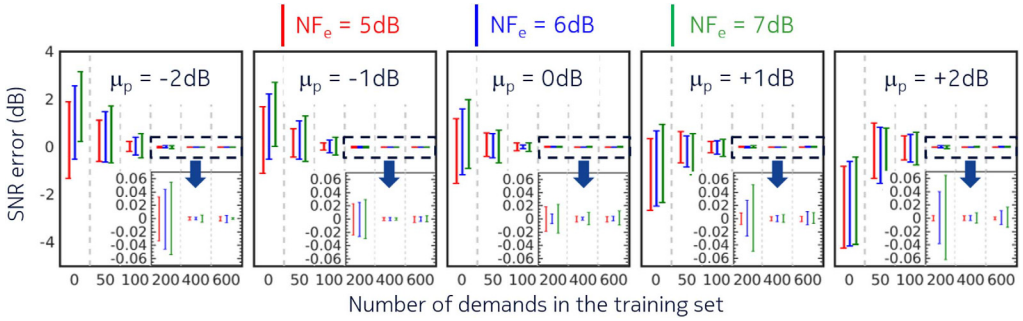

Fig. 8. Range of the SNR prediction error (mean ± 3σ) for one demand among all the remaining demands as a function of the number of demands N_d in the training set and for five values of systematic power shift μ_p: −2 to +2 dB. The three error bars for each size of the training set correspond to various estimated noise figures NF_e:5, 6, and 7 dB, respectively (left to the right). Zero demand means there is no training (QoT model: EGN).

EGN model. Expanding this method could help further reduce overprovisioning and thus the cost of optical network equipment.

Acknowledgment

This work was partly supported by the H2020 EU project ORCHESTRA under Grant 645360. This paper is an extended version of Ref. [26].

References

[1] A. Mitra, A. Lord, S. Kar, and P. Wright, "Effect of link margin and frequency granularity on the performance of a flexgrid optical network," *Opt. Express*, vol. 22, no. 1, pp. 41–46, Jan. 2014.

[2] J. Pesic, T. Zami, N. Rossi, and S. Bigo, "Do elastic transponders with granularity finer than 50 Gb/s make gradual fit of modulation to ageing more profitable?" in *Optical Fiber Communication Conf. (OFC)*, March 2017, paper W1I4.

[3] M. O'Sullivan, "Machine learning applied to subsystems," in *Optical Fiber Communication Conf. (OFC)*, March 2017.

[4] Y. Pointurier, "Design of low-margin optical networks (Invited)," in *Optical Fiber Communication Conf. (OFC)*, March 2016, paper Tu3F5.

[5] J.-L. Augé, "Can we use flexible transponders to reduce margins?" in *Optical Fiber Communication Conf. (OFC)*, March 2013, paper OTu2A.1.

[6] "Intelligent optical networks: A look into the future," [Online]. Available: https://www.youtube.com/watch?v=eJFHFRRQvrs.

[7] Coriant, "Evolving the awareness of optical networks," White Paper, 2017 [Online]. Available: http://www.coriant.com/spotlights/aware-white-paper.asp.

[8] Ciena, "Transforming margin into capacity with liquid spectrum," White Paper, 2017 [Online]. Available: www.ciena.com/insights/white-papers/Margin-Capacity-Liquid-Spectrum-prx.html.

[9] Y. Nozu, Y. Aoki, K. Komaki, and S. Okano, "'Conscious optical network' with reliability and flexibility," *Fujitsu Sci. Tech. J.*, vol. 52, no. 2, pp. 75–82, April 2016.

[10] L. Barletta, A. Giusti, C. Rottondi, and M. Tornatore, "QoT estimation for unestablished lightpaths using machine learning," in *Optical Fiber Communication Conf. (OFC)*, March 2017, paper Th1J1.

[11] J. Wass, J. Thrane, M. Piels, R. Jones, and D. Zibar, "Gaussian process regression for WDM system performance prediction," in *Optical Fiber Communication Conf. (OFC)*, March 2017, paper Tu3D7.

[12] P. Poggiolini, "The GN model of non-linear propagation in uncompensated coherent optical systems," *J. Lightwave Technol.*, vol. 30, no. 24, pp. 3857–3879, 2012.

[13] E. Grellier and A. Bononi, "Quality parameter for coherent transmissions with Gaussian-distributed nonlinear noise," *Opt. Express*, vol. 19, no. 13, pp. 12781–12788, 2011.

[14] R. Dar, M. Feder, A. Mecozzi, and M. Shtaif, "Properties of nonlinear noise in long, dispersion-uncompensated fiber links," *Opt. Express*, vol. 21, no. 22, pp. 25685–25699, Nov. 2013.

[15] A. Carena, G. Bosco, V. Curri, Y. Jiang, P. Poggiolini, and F. Forghieri, "EGN model of non-linear fiber propagation," *Opt. Express*, vol. 22, no. 13, pp. 16335–16362, 2014.

[16] P. Johannisson and E. Agrell, "Modeling of nonlinear signal distortion in fiber-optic networks," *J. Lightwave Technol.*, vol. 32, no. 23, pp. 4544–4552, 2014.

[17] B. Lavigne, M. Lefrançois, E. Balmefrezol, C. Bresson, F. Vacondio, J.-C. Antona, E. Seve, and O. Rival, "System design tool for high bit rate terrestrial transmission systems with coherent detection," *Bell Labs Tech. J.*, vol. 18, no. 3, pp. 251–266, 2013.

[18] E. Seve, P. Ramantanis, J.-C. Antona, E. Grellier, O. Rival, F. Vacondio, and S. Bigo, "Semi-analytical model for the performance estimation of 100 Gb/s PDM-QPSK optical transmission systems without inline dispersion compensation and mixed fiber types," in *European Conf. on Optical Communication (ECOC)*, Sept. 2013, paper Th.1D2.

[19] N. Sambo, Y. Pointurier, F. Cugini, L. Valcarenghi, P. Castoldi, and I. Tomkos, "Lightpath establishment assisted by offline QoT estimation in transparent optical networks," *J. Opt. Commun. Netw.*, vol. 2, no. 11, pp. 928–937, Nov. 2010.

[20] I. Sartzetakis, K. Christodoulopoulos, C. P. Tsekrekos, D. Syvridis, and E. Varvarigos, "Quality of transmission in WDM and elastic optical networks accounting for space-spectrum dependencies," *J. Opt. Commun. Netw.*, vol. 8, no. 9, pp. 676–688, Aug. 2016.

[21] S. Oda, M. Miyabe, S. Yoshida, T. Katagiri, Y. Aoki, T. Hoshida, J. C. Rasmussen, M. Birk, and K. Tse, "A learning living network with open ROADMs," *J. Lightwave Technol.*, vol. 35, no. 8, pp. 1350–1356, Apr. 2017.

[22] M. Bouda, S. Oda, O. Vasilieva, M. Miyabe, S. Yoshida, T. Katagiri, Y. Aoki, T. Hoshida, and T. Ikeuchi, "Accurate prediction of quality of transmission with dynamically configurable optical impairment model," in *Optical Fiber Communication Conf. (OFC)*, March 2017, paper Th1J4.

[23] P. Poggiolini, G. Bosco, A. Carena, V. Curri, Y. Jiang, and F. Forghieri, "A detailed analytical derivation of the GN model of non-linear interference in coherent optical transmission systems," arXiv.org:1209.0394, 2014.

[24] P. Jennevé, P. Ramantanis, F. Boitier, N. Dubreuil, and S. Bigo, "Experimental investigation of the validity domain of the Gaussian noise model over dispersion managed systems," in *Optical Fiber Communication Conf. (OFC)*, March 2016, paper W3I3.

[25] http://sndlib.zib.de/home.action.

[26] E. Seve, J. Pesic, C. Delezoide, and Y. Pointurier, "Learning process for reducing uncertainties on network parameters and design margins," in *Optical Fiber Communication Conf. (OFC)*, March 2017, paper W4F6.

Emmanuel Seve received a Ph.D. in physics from Bourgogne University, France. Between 1999 and 2000, he was a postdoctoral fellow at Aston University in Birmingham, UK. In July 2000, he joined Alcatel (then Alcatel–Lucent and now Nokia) Bell Labs as a research engineer. His primary research was focusing on physical impairment modeling and now its application on optical and intelligent network modeling.

Jelena Pesic received a Ph.D. from the University of Bretagne Sud in collaboration with France Telecom–Orange Labs, France, in 2012. From 2012 to 2014, she was a postdoctoral fellow at INRIA and Telecom Bretagne working on the European project SASER. She received a best paper award at the IEEE ONDM conference in 2011. After joining Alcatel–Lucent (now Nokia) Bell Labs in 2014, she focused on dynamic elastic networks dimensioning and techno-economic studies. Her main areas of research interest include intelligent optical networks, including core and metro networks.

Camille Delezoide received an engineer degree and M.S. in optics and photonics from the Institut d'Optique Graduate School, Palaiseau, France, in 2007 and a Ph.D. from Ecole Normale Supérieure Paris-Saclay, Cachan, France, in 2012. He spent two years as a postdoctoral fellow at the Laboratoire de Photonique Quantique et Moléculaire (LPQM) in Cachan studying microresonator-based biosensing. He joined Alcatel–Lucent (now Nokia) Bell Labs as a research engineer in 2014. He is currently the Bell Labs coordinator for the ORCHESTRA H2020 research project. His current research interests are flexible optical networks, software-based optical performance monitoring, and network optimization.

Sébastien Bigo (SM13, FM17) graduated from the Institut d'Optique Graduate School in 1992. In 1996, he received a Ph.D. in physics for work devoted to all-optical processing and soliton transmission. He joined Alcatel Research & Innovation (now Nokia Bell Labs) in 1993, while a student at the University of Besançon, France. In 1997, he started studying high-capacity WDM transmission systems, and conducted large-scale demonstration experiments, at 10 Gb/s, 40 Gb/s, 100 Gb/s, and 400 Gb/s channel rates. He is currently heading the Optical Networks Department. He has authored and co-authored more than 300 journal and conference papers and 40 patents. He has been a Bell Labs Fellow since 2012. He received the General Ferrié Award in 2003 from the French ICT society, the IEEE/SEE Brillouin Award in 2008, and the Marius–Lavet Inventor–Engineer Award in 2010 and 2017. He was elected Governor of the IEEE Photonics Society from 2012 to 2014.

Yvan Pointurier (S02, M06, SM12) received a Ph.D. from the University of Virginia, USA, in 2006. Between 2006 and 2009, he was a postdoctoral fellow at McGill University in Montreal, and then a senior researcher at AIT, Greece. In 2009, he joined Alcatel–Lucent (now Nokia) Bell Labs as a research engineer, and is now the head of the Dynamic Optical Networking and Switching Department at Nokia Bell Labs. His team is working on circuit and optical packet-switched networks, with activities ranging from the physical layer to planning algorithms. He has authored or co-authored more than 15 European and US patents and over 90 technical papers in leading journals, key conferences (OFC, ECOC, ACM Internet Measurement Conference, IEEE INFOCOM, ICC, and GLOBECOM), and book chapters. He received a best paper award at the IEEE ICC conference in 2006 and an *IEEE Communication Letters* Exemplary Reviewer award between 2014 and 2016 (top 3% of the reviewers). He has been a TPC member for IEEE ICC, the flagship IEEE conference on communications, since 2007. He is currently the French coordinator for the CELTIC+SENDATE-TANDEM project, a 36-month, 2200 person-month project led by Nokia Bell Labs.